IMMUNOLOGY

Blockade of surface-bound TGF-β on regulatory T cells abrogates suppression of effector T cell function in the tumor microenvironment

Sadna Budhu,[1,2]* David A. Schaer,[1]* Yongbiao Li,[3] Ricardo Toledo-Crow,[3] Katherine Panageas,[4] Xia Yang,[1,2] Hong Zhong,[1,2] Alan N. Houghton,[1] Samuel C. Silverstein,[5] Taha Merghoub,[1,2†] Jedd D. Wolchok[1,2,6†]

Regulatory T cells (T$_{regs}$) suppress antitumor immunity by inhibiting the killing of tumor cells by antigen-specific CD8$^+$ T cells. To better understand the mechanisms involved, we used ex vivo three-dimensional collagen-fibrin gel cultures of dissociated B16 melanoma tumors. This system recapitulated the in vivo suppression of antimelanoma immunity, rendering the dissociated tumor cells resistant to killing by cocultured activated, antigen-specific T cells. Immunosuppression was not observed when tumors excised from T$_{reg}$-depleted mice were cultured in this system. Experiments with neutralizing antibodies showed that blocking transforming growth factor–β (TGF-β) also prevented immunosuppression. Immunosuppression depended on cell-cell contact or cellular proximity because soluble factors from the collagen-fibrin gel cultures did not inhibit tumor cell killing by T cells. Moreover, intravital, two-photon microscopy showed that tumor-specific Pmel-1 effector T cells physically interacted with tumor-resident T$_{regs}$ in mice. T$_{regs}$ isolated from B16 tumors alone were sufficient to suppress CD8$^+$ T cell–mediated killing, which depended on surface-bound TGF-β on the T$_{regs}$. Immunosuppression of CD8$^+$ T cells correlated with a decrease in the abundance of the cytolytic protein granzyme B and an increase in the cell surface amount of the immune checkpoint receptor programmed cell death protein 1 (PD-1). These findings suggest that contact between T$_{regs}$ and antitumor T cells in the tumor microenvironment inhibits antimelanoma immunity in a TGF-β–dependent manner and highlight potential ways to inhibit intratumoral T$_{regs}$ therapeutically.

INTRODUCTION

It is well established that the immune system is capable of recognizing and eliminating neoplastic tumor growth; however, subsequent editing of the tumor by the immune system and other suppressive mechanisms enable tumors to escape further immune-mediated destruction (1, 2). In addition to rendering the immune system ignorant to their presence, tumors can alternatively use more active processes to suppress anti-tumor immunity. Although several types of inhibitory cells [such as regulatory T cells (T$_{regs}$), myeloid-derived suppressor cells, and natural killer T cells] infiltrate B16 melanoma tumors during their growth, it is well established that T$_{regs}$ contribute to inhibition of the antitumor immune response (3–5). The efficacy of many immunotherapeutic approaches that target T cell co-inhibitory and costimulatory receptors correlates with an altered balance in the ratio of effector T cells to T$_{regs}$ in favor of the effector cells (3, 6, 7). Despite the evidence that T$_{regs}$ inhibit antimelanoma immunity, the question remains as to where and through what mechanism T$_{regs}$ inhibit the antitumor immune response. T$_{regs}$ can inhibit tumor antigen–specific T cell responses through several mechanisms, including the release of suppressive cytokines [such as transforming growth factor–β (TGF-β), interleukin-10 (IL-10), and IL-35], consumption of IL-2, lysis of effector cells through granzyme

and perforin, attenuation of antigen-presenting cells (APCs) through the inhibitory molecule cytotoxic T lymphocyte–associated protein 4 (CTLA-4), hydrolysis of extracellular adenosine triphosphate by CD39, and activation of cyclic adenosine monophosphate (cAMP), inducible cAMP early repressor, and nuclear factor of activated T cells (8). The mechanisms that T$_{regs}$ use to suppress effector cells are context-dependent, and factors such as target cell type, site of inflammation, and the activation states of the target cells and T$_{regs}$ can influence the suppression. Additionally, it appears that T$_{regs}$ must come into direct contact with effector T cells to suppress T cell receptor (TCR) signaling and that this suppressive state in the effector cells is maintained even when T$_{regs}$ are removed from cocultures (9).

One fundamental question regarding T$_{reg}$-mediated suppression is whether T$_{regs}$ suppress the priming of naïve, tumor antigen–specific T cells in the tumor-draining lymph node (TDLN) or the effector phase of the T cell responses in the tumor microenvironment. Evidence exists that tumor antigen–specific T cells can be primed in vivo in secondary lymphoid organs and that these activated cells can be found within tumors. We previously reported that melanoma antigen (gp100)–specific TCR transgenic CD8$^+$ T cells (Pmel-1 CD8$^+$ T cells) are efficiently primed and activated in B16 tumor–bearing animals (10). Although adoptively transferred Pmel-1 CD8$^+$ T cells demonstrate peripheral cytolytic ability and display intratumor, antigen-specific recognition of cognate tumor targets, they are unable to induce tumor regression (10). Similar observations were obtained from experiments with OT-1 TCR transgenic CD8$^+$ T cells and B16 tumors expressing a strong foreign antigen ovalbumin (B16-OVA), showing that the strength of antigens is not responsible for the observed result (10).

Here, we describe an ex vivo assay that recapitulates the suppressive effects of the tumor microenvironment in vivo. We showed that T$_{regs}$ from B16 tumors suppressed the killing of explanted tumor cells by

antigen-specific CD8^{+} T cells in a contact-dependent manner. The suppressed CD8^{+} T cells had reduced amounts of granzyme B and increased amounts of the inhibitory protein programmed cell death protein 1 (PD-1) compared to those of nonsuppressed CD8^{+} T cells. Moreover, neutralizing antibodies against surface-bound TGF-β on T_{regs} blocked the suppression and restored CD8^{+} T cell–mediated killing of tumor cells. These data suggest that targeting T_{regs} (with anti–TGF-β antibodies or other immunotherapies) in vivo might provide therapeutic benefit in a clinical setting.

RESULTS

Ex vivo three-dimensional collagen-fibrin gel cultures maintain the immunosuppression present in the tumor microenvironment

T_{regs} play an important role in suppressing antimelanoma immunity (4, 5). To investigate whether T_{regs} in mouse melanomas mediate suppression of cytotoxic T cells in the tumor microenvironment, we used a previously described ex vivo three-dimensional (3D) collagen-fibrin gel coculture killing assay (11). Collagen-fibrin gel cultures in combination with a clonogenic assay for assessing viable melanoma cells can enable precise measurement of the efficiency of killing of B16 melanoma tumor cells by CD8^{+} T cells. This cytotoxicity assay mimics a 3D tissue-like environment. In addition, the cultures are stable over long periods of time, which enables the assessment of CD8^{+} T cell killing of melanoma cells over several days.

We implanted B16-OVA cells intradermally on the flanks of C56BL/6 mice and isolated tumors 10 days after inoculation. After excision, tumors were mechanically dissociated into single-cell suspensions (Fig. 1A). The numbers of viable tumor cells and infiltrating immune cells were assessed by trypan blue exclusion. Dissociated B16-OVA tumor cells were co-embedded with in vitro–activated OT-1 T cells (TCR transgenic CD8^{+} T cells specific for OVA_{257-64}) at a T cell–to–viable tumor cell ratio of 50:1. Twenty-four, 48, and 72 hours later, the gels were enzymatically dissolved with collagenase and trypsin, and the numbers of remaining viable tumor cells were quantified by plating the cells and analyzing colony formation (Fig. 1A). In this setting, the colony counts reflect the number of remaining viable tumor cells that resisted killing by T cells. OT-1 cells kill B16-OVA cells continuously at an exponential rate (11). This can be schematically represented as a negative-sloped straight line on a semilog plot of viable tumor cells (Fig. 1B). If there is less killing (or if killing is suppressed), the slope of the line becomes more positive (Fig. 1C). When there are no T cells present in these gels, the tumor cells will continue to grow exponentially over time, which can be

schematically illustrated by a positive-sloped straight line (Fig. 1, B and C). In addition, a previously described equation (Fig. 1D) is used to calculate the killing efficiency of the CD8^{+} T cells, which is represented by the killing constant k in this equation.

Using this approach, we first established whether ex vivo collagen gel cultures could recapitulate the immunosuppression that occurs in B16 tumors in vivo. In vitro–activated effector OT-1 CD8^{+} T cells (5×10^5 viable cells per gel) were cocultured in collagen-fibrin gels with either tissue-cultured B16-OVA cells (1×10^4 viable cells per gel) or single-cell suspensions of dissociated B16-OVA tumors (1×10^4 viable tumor cells per gel). Note that the dissociated B16 tumors generally contained about threefold more viable (trypan blue–negative) infiltrating immune cells than viable tumor cells (Fig. 2A), similar to what was previously reported (10). These cultures were incubated for 24 and 48 hours, after which the numbers of remaining viable melanoma cells were determined using a clonogenic assay. Consistent with a previous report (11), tissue-cultured B16 cells were continuously killed over time when cocultured with OT-1 cells (Fig. 2B, left). OT-1 cells killed dissociated B16-OVA tumor cells and cultured B16-OVA cells equivalently within the first 24 hours in the collagen-fibrin gels; however, after 24 hours, killing of the dissociated tumor cells was markedly reduced. Dissociated B16-OVA tumor cells began to grow in the gels at a similar rate to that of tumor cells alone (Fig. 2B,
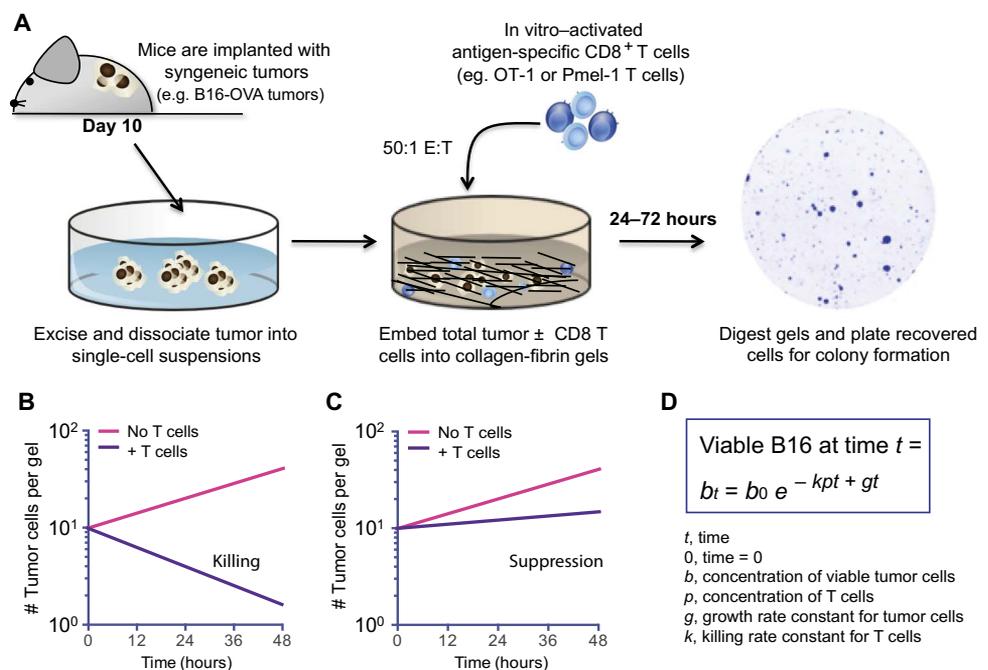

Fig. 1. Schematic representation of the experimental setup for the 3D collagen-fibrin gel killing assay. (A to D) Illustration and representation of the model and technique used in this study. (A) Melanoma tumors expressing the T cell antigens OVA and Pmel-1 (B16-OVA) are excised from C57BL/6 mice 10 days after implantation and dissociated into single-cell suspensions. Collagen-fibrin gels are prepared in 48-well tissue culture plates containing B16-OVA cells from in vitro culture or B16-OVA cells from the dissociated tumors in the presence or absence of antigen-specific CD8^{+} T cells. The gels are lysed daily with collagenase and trypsin, and the numbers of remaining viable B16-OVA cells are assessed with a clonogenic assay as previously described (11). (B to D) Illustration of the use of the 3D collagen-fibrin gel killing assay to qualitatively measure the suppression of T cell killing by the tumor microenvironment with hypothetical representation of semilog plots showing the expected numbers of viable B16 cells recovered from collagen-fibrin gels in which T cell–mediated killing (B) or immunosuppression of killing (C) occurred. (D) Equation modeling the T cell–mediated killing of tumor cells in collagen-fibrin gels to calculate the killing efficiency, k, as previously described (11).

In the figure equation box (Fig. 1D):

Viable B16 at time t =
$$b_t = b_0\, e^{-kpt + gt}$$

t, time
0, time = 0
b, concentration of viable tumor cells
p, concentration of T cells
g, growth rate constant for tumor cells
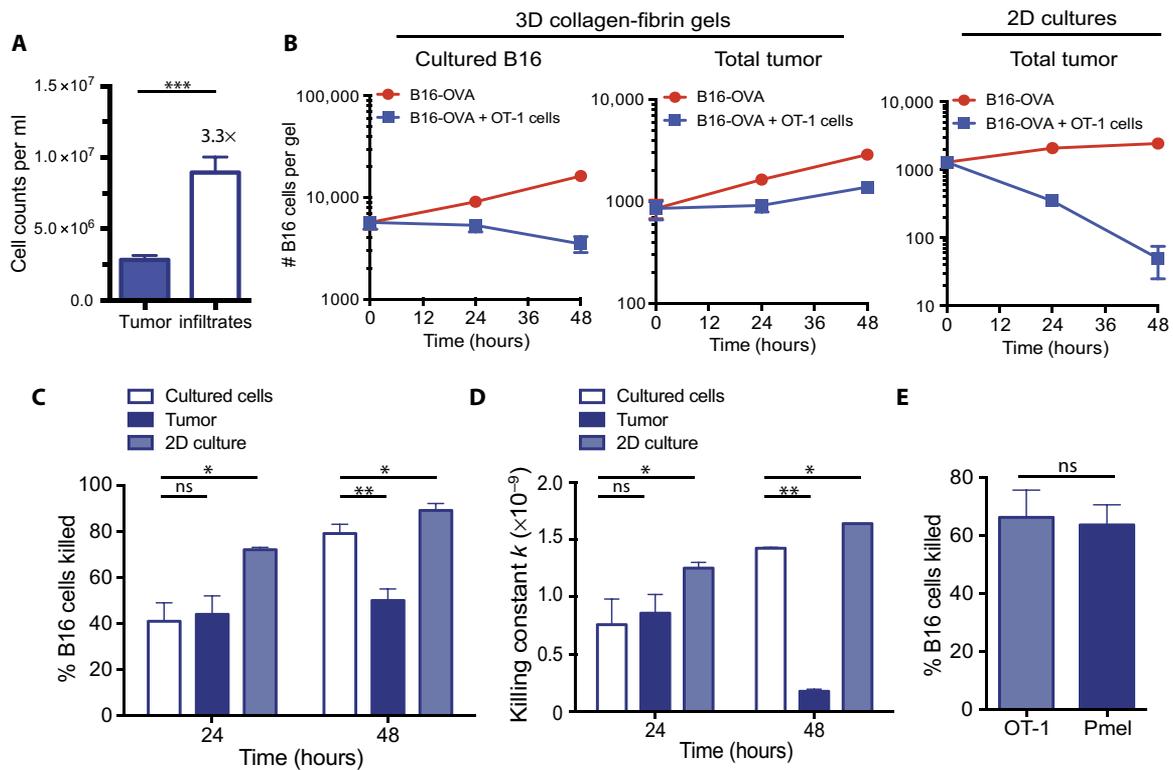k, killing rate constant for T cells

Fig. 2. Ex vivo collagen-fibrin gel cultures maintain the immunosuppression of in vivo tumor microenvironment. (A to E) B16-OVA tumors were excised and digested with collagenase and then disaggregated mechanically into single-cell suspensions. Dissociated tumors were co-embedded in collagen-fibrin gels with in vitro–activated OT-1 cells at a 50:1 effector-to-target (E:T) ratio. (A) The numbers of viable tumor cells and immune cell infiltrates isolated from dissociated 10-day B16-OVA tumors were determined. Data are means ± SEM of eight experiments. (B) The numbers of viable melanoma cells recovered from the gels at the indicated times were measured. Data are means ± SEM of three independent experiments performed in duplicate. (C) The percentages of B16 cells killed were determined. Data are means ± SEM of eight experiments as performed in (A). (D) Calculated value of k ± SEM from the experiments performed in (A) using the equation $b_t = b_0 e^{-kpt+gt}$, as described in Materials and Methods. (E) The percentages of B16 tumor cells killed were determined. Data are means ± SEM at 24 hours using equivalent numbers (5×10^5 cells per gel) of OT-1 or Pmel CD8+ T cells in collagen-fibrin gel cocultures of B16-OVA cells. *$P \leq 0.05$, **$P \leq 0.01$, and ***$P \leq 0.005$. ns, not significant.

middle). This suppression of cell killing resulted in a 34% decrease in the percentage of dissociated B16-OVA tumor cells that were killed compared to the cultured B16-OVA cells at the 48-hour time point (Fig. 2C), with an eightfold decrease in the killing efficiency of the CD8+ T cells as measured by the killing rate constant k (Fig. 2D). Similar results were obtained from experiments with CD8+ T cells from a TCR transgenic mouse that recognizes the melanoma antigen gp100 (Pmel-1 CD8+ T cells), which showed that killing rates and the suppression of killing were not dependent on antigen strength (Fig. 2E).

Because dissociated tumors contain not only tumor cells but also infiltrating lymphocytes and stromal components, these findings suggested that cells present in the dissociated tumors and any factors they produced suppressed the cytolytic activity of the CD8+ T cells. In addition, we found that maintenance of the suppressive environment was dependent on the presence of collagen and fibrin because 2D cultures of the same dissociated B16-OVA tumors failed to recapitulate the suppression observed in the gels (Fig. 2B, right). In these 2D cultures, the dissociated B16-OVA tumor cells were killed more efficiently than were the tissue-cultured B16-OVA cells (Fig. 2, C and D). These data suggested that the 3D extracellular matrix surrounding the tumors plays an important role in supporting the immunosuppressive tumor microenvironment.

In vivo depletion of T_{regs} in Foxp3-DTR mice results in loss of ex vivo immunosuppression

Having established that 3D collagen-fibrin gels recapitulated the type of immunosuppression observed in tumors in vivo, we examined whether T_{regs} were responsible for suppressing CD8+ T cells in the tumor microenvironment. We implanted Foxp3-DTR mice [transgenic mice with diphtheria toxin (DT) receptor (DTR) expression driven by the *Foxp3* promoter] (4) with B16-OVA tumors to deplete T_{regs} before tumor excision. A single dose (45 ng) of DT was injected 9 days after tumor implantation, and the tumors were excised 2 days thereafter. This treatment schedule was optimized to deplete the maximum number of T_{regs} (range, 60 to 85%) in Foxp3-DTR mice without having a statistically significant effect on other immune cell populations within the tumor (fig. S1) (4). Treatment with DT completely abolished the suppression observed compared to control tumors excised from either wild-type (WT) mice or nontreated littermate control Foxp3-DTR mice (Fig. 3A). The amount of killing observed was comparable to that of cultured B16 cells, although T_{regs} were not completely depleted from tumors with this treatment regimen (Fig. 3, A and B). In addition, calculation of the killing constant k and the percentage of B16 cells killed showed that the killing efficiency of OT-1 cells in the T_{reg}-depleted tumors was similar to that of cultured B16 cells where there were no suppressive cells present (Fig. 3, C and D).
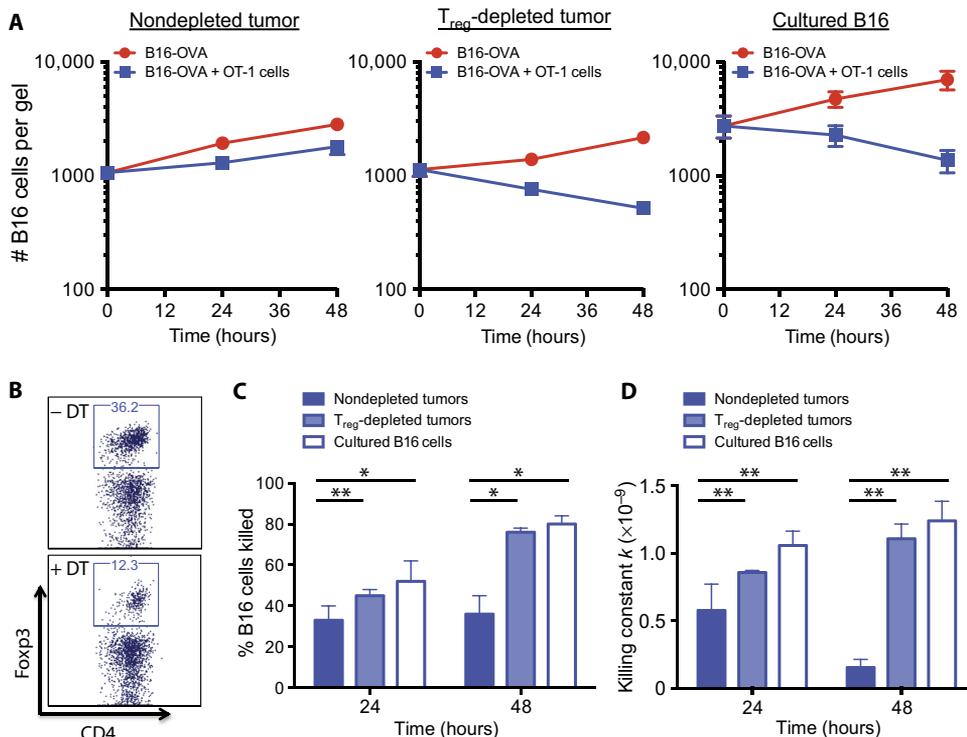
Fig. 3. In vivo depletion of T$_{regs}$ in Foxp3-DTR mice restores CD8$^+$ T cell–mediated tumor cell killing. (A to D) Foxp3-DTR mice were treated with DT to deplete T$_{regs}$ 2 days before tumor excision was performed, as described in Materials and Methods. The dissociated tumors were co-embedded in collagen-fibrin gels with in vitro–activated OT-1 cells at a 50:1 effector-to-target ratio. **(A)** At the indicated times, the gels were dissolved, and the numbers of remaining B16 cells were measured using a clonogenic assay. Data are means of the number of viable B16 cells ± SEM from three experiments performed in duplicate. **(B)** Representative plots (gated on viable CD45$^+$ immune cells) of CD4$^+$Foxp3$^+$ T$_{regs}$ in B16-OVA tumors with or without DT treatment. **(C)** The percentages of B16 cells killed under the indicated conditions were determined. Data are means ± SEM from three experiments performed in duplicate as described in (A). **(D)** Mean values of k ± SEM from the experiments performed in (A). *$P \leq 0.05$ and **$P \leq 0.01$.

of tumor cells by CD8$^+$ T cells (fig. S3A). Similar observations were made using the anti–CD25-depleting antibody (PC61) in vivo in a B16-OVA tumor model in which a 40 to 50% depletion of intratumoral T$_{regs}$ was achieved, and no tumor regression was observed (5). Furthermore, the addition of T$_{regs}$ purified with anti-CD25 magnetic beads to the collagen-fibrin gel cultures did not suppress OT-1 cell–mediated killing of cultured B16-OVA cells (fig. S3B). Further support for this finding came from a study that showed that treatment with a glucocorticoid-induced tumor necrosis factor receptor (TNFR)–related protein (GITR) agonist antibody (DTA-1), which can both deplete intratumoral T$_{regs}$ and induce lineage instability in the remaining T$_{regs}$ such that they are no longer suppressive, restored the ex vivo killing of B16 tumors similarly to DT treatment in Foxp3-DTR mice (13). This suggests that although intratumoral T$_{regs}$ are responsible for the suppression of CD8$^+$ T cell–mediated killing observed in our studies, they need to be depleted sufficiently or rendered nonsuppressive.

Blocking TGF-β reverses the ex vivo immunosuppression by the tumor microenvironment

T$_{regs}$ can suppress immune responses through the secretion of soluble factors, such as IL-10, TGF-β, and IL-35, or through cell-cell contact and, possibly, direct killing of target cells (14–16). Intervention in these suppressive pathways by either genetic disruption of the receptors or through neutralizing antibodies delays melanoma tumor growth, but their contribution to the tumor microenvironment has not been delineated (17). Using blocking antibodies in collagen-fibrin gel cultures, we asked whether any of these factors contributed to the T$_{reg}$-mediated suppression observed in the tumor microenvironment. The addition of blocking antibodies against the IL-10 receptor (IL-10R) and IL-35 had no effect on the suppression observed in dissociated B16 tumors in the collagen-fibrin cultures (Fig. 4, A and B). However, blocking TGF-β reversed suppression and restored OT-1 cell killing efficiency to a similar rate as that observed with cultured B16-OVA cells and T$_{reg}$-depleted tumors (Figs. 3, C and D, and 4, A and B). Blocking TGF-β had no effect on the growth of dissociated B16-OVA cells in the absence of OT-1 T cells nor did it affect the growth or killing of cultured B16 cells in collagen-fibrin gels (Fig. 4C). T$_{reg}$-mediated suppression did not appear to be dependent on TCR engagement by T$_{regs}$ in the cultures because blocking major histocompatibility complex (MHC) II did not restore tumor killing (Fig. 4, A and B).

T$_{regs}$ interact with tumor-specific Pmel-1 T cells within B16 tumors

Considering that depletion of T$_{regs}$ alters melanoma tumor growth in vivo and removes the suppression of CD8$^+$ T cell–mediated killing

T$_{regs}$ represent a small portion of the total cells within the tumor microenvironment, but it is possible that inducing apoptosis alone through DTR engagement could alter the tumor microenvironment, making the tumor susceptible to killing in the collagen-fibrin gels. To rule out this possibility, we performed a control experiment in which we depleted a subset of myeloid cells (which represent a larger portion of the tumor stroma than do T$_{regs}$) using CCR2-DTR mice (12). CCR2 is expressed primarily on the monocytic CD11b$^+$ myeloid population within tumors, and it was previously shown that depleting CCR2$^+$ cells with DT in the B16 melanoma model does not affect tumor growth in vivo (12). Consistent with previous data, we found that CCR2-depleted tumors remained suppressive in the ex vivo collagen-fibrin gels (fig. S2).

Although DT treatment of Foxp3-DTR mice depleted 60 to 85% of the T$_{regs}$ in the tumors in vivo, examination of the T$_{regs}$ remaining in collagen-fibrin gels showed that the percentage of T$_{regs}$ continued to decrease over time. This suggests that in vivo treatment with DT continued to modulate the ability of the remaining T$_{regs}$ to suppress killing. We found that simply reducing the number of T$_{regs}$ ex vivo by other means was insufficient to reduce suppression. We used anti-CD25 magnetic beads to deplete T$_{regs}$ from tumor cell suspensions ex vivo. This method reduced the number of T$_{regs}$ by 50 to 60% in the dissociated tumors; however, it was not sufficient to restore the killing
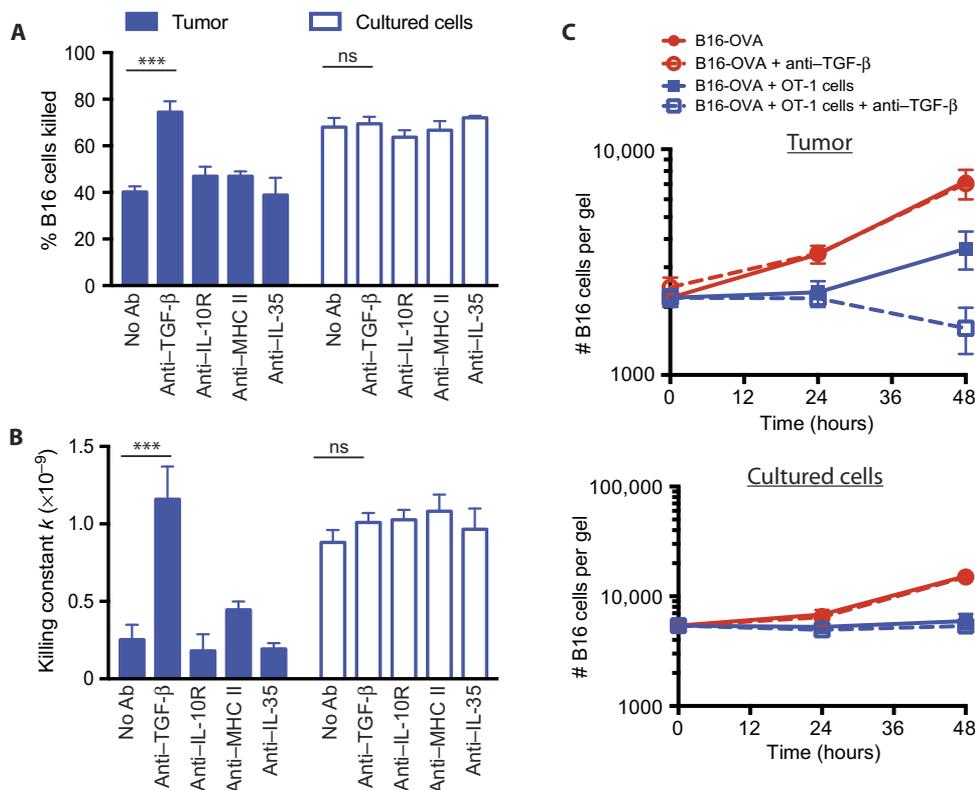
Fig. 4. TGF-β blockade reverses the suppression of tumor cell killing ex vivo. (A to C) B16-OVA tumors were excised and dissociated as described in Fig. 2. The dissociated tumors were co-embedded in collagen-fibrin gels with in vitro–activated OT-1 cells at a 50:1 effector-to-target ratio in the presence or absence of blocking antibodies (Ab) against TGF-β, IL-10R, MHC II, or IL-35 (all at 10 μg/ml). (A) The percentages of B16 cells killed at 48 hours were determined. Data are means ± SEM of three experiments performed in duplicate. (B) The mean values of k ± SEM from the experiments performed in (A) were determined. (C) The mean numbers of clonogenic B16 remaining at the indicated times were determined. Data are means ± SEM of three experiments performed in duplicate. ***$P \leq 0.005$.

apparent that many CFP-Pmel T cells were in close proximity to, or came into contact with, Foxp3-GFP T_{regs} during the imaging periods (Fig. 5A, inset, and movie S2).

To quantify the duration of these interactions, we generated a weighted score for both contact and proximity at each time point for each Pmel-1 T cell tracked for at least 10 time points (see Materials and Methods). More than 40% of the visualized Pmel-1 T cells demonstrated either proximity to (within 10 μm) or contact with T_{regs}. As a total population, Pmel-1 T cells spent 10% of their time in contact and 25% of their time within 10 μm of T_{regs} inside YFP-B16 tumors (Fig. 5B). On average, Pmel-1 T cells that had at least one interaction with a T_{reg} were found in contact or in proximity to T_{regs} 25 and 68% of the time, respectively. However, we did not observe any substantial differences between interaction scores and Pmel-1 mobility within the tumor microenvironment, similar to what has been previously reported in lymph nodes (LNs) (fig. S4A) (18). There was a small but statistically significant ($P < 0.005$) increase in the area of movement in T cells that interacted with T_{regs} compared to those that did not (fig. S4B). Although T_{regs} are thought to suppress T cell effector function within the tumor microenvironment, it appeared that they did not do so by decreasing the motility of the effector cells.

ex vivo, it seems logical that T_{regs} are the root cause of intratumoral immunosuppression (4, 5, 10). It was previously demonstrated that infiltration of CD8+ T cells within the tumor microenvironment coincides with an enriched recruitment of T_{regs} compared to the periphery (10). Although T_{regs} and effector T cells colocalize to the same regions of B16 tumors, little is known about the interactions that take place between these two populations. Because T_{regs} control immune responses in a contact-dependent manner (18, 19), we examined whether any interactions occurred between tumor-specific CD8+ T cells and T_{regs} within B16 tumors. Through an intravital imaging model of B16 melanoma, Foxp3–green fluorescent protein (GFP) fusion knock-in transgenic mice were implanted with yellow fluorescent protein–expressing B16 melanoma cells (YFP-B16) (10, 20). Three days after tumor implantation, naïve cyan fluorescent protein–expressing Pmel-1 CD8+ T cells (CFP-Pmel) were adoptively transferred into the Foxp3-GFP tumor-bearing mice. Tumors were then imaged starting 7 days after the adoptive transfer of the CFP-Pmel cells (day 10 of tumor growth) as previously described (10). This procedure enabled visualization of the interactions between CFP-Pmel T cells and Foxp3-GFP T_{regs} in the context of the YFP-B16 tumor. CFP-Pmel T cells were consistently found in regions highly infiltrated by T_{regs} (Fig. 5A and movie S1). Upon close examination, it was

T_{regs} suppress CD8+ T cell effector function through surface-bound TGF-β

Given the observation that T_{regs} were proximal to and interacted with CD8+ T cells within the tumor microenvironment in vivo (Fig. 5), we assessed how important these interactions were for the ability of T_{regs} to suppress tumor cell killing. Because both contact-dependent and soluble mechanisms have been described for TGF-β–mediated suppression by T_{regs} (14, 21), we investigated whether suppression in dissociated tumors could be transferred from a nondepleted tumor to T_{reg}-depleted tumors (19, 22). Collagen-fibrin gels containing single-cell suspensions from T_{reg}-depleted tumors and OT-1 cells were placed in the upper compartment of 24-well cell culture inserts, and collagen-fibrin gels containing nondepleted tumors were added to the bottom of the 24-well plates (fig. S5A). If soluble factors secreted from the tumor cells or their infiltrates were responsible for the suppression, then we would expect to observe the inhibition of killing after 24 hours. Examination of the viable tumor cells remaining in the inserts after 24 to 48 hours in culture showed that OT-1 cells continued to kill tumor cells, suggesting that suppression was not transferable (fig. S5, B and C). These data suggest that T_{regs} either inhibit CD8+ T cell cytotoxicity through surface-bound TGF-β or produce soluble TGF-β that can only exert its effect within the close proximity observed inside the tumor microenvironment. In
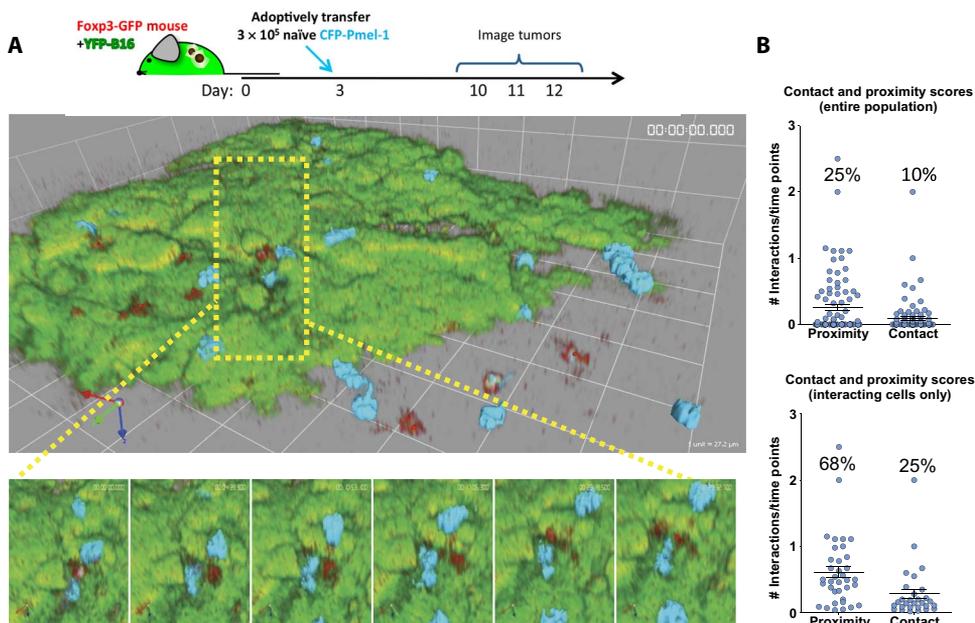
Fig. 5. Pmel-1 T cells are located near to and interact with T_regs in YFP-B16 tumors. (**A** and **B**) YFP-B16 tumor cells were suspended in Matrigel and inoculated subcutaneously into Foxp3-GFP mice. Three days later, 3×10^5 naïve CFP-Pmel CD8$^+$ T cells were transferred by tail vein injection. The mice were then imaged as described in Materials and Methods. Time-lapse images were analyzed for the interactions of CD8$^+$ CFP-Pmel T cells (cyan) with T_regs (red) as described in Materials and Methods. (A) Top: Representative frames from a single region of a six-region time-lapse image. Bottom: Magnified images from the region surrounded by the yellow box. Foxp3-GFP T_regs are depicted in red, CFP-Pmel cells are depicted in cyan, and YFP-B16-OVA tumor cells are depicted in green. Frames are separated in time by 6 min 12 s. (B) Points on plots represent individual cells scored for proximity (within 10 µm) or contact with a T_reg during imaging (see Materials and Methods). Top: Data are means ± SEM of the entire population of cells. Bottom: Data are means ± SEM of only those cells that had interactions with T_regs. All cells tracked for over five time points from four mice are represented.

producing TGF-β and the α_V integrin (CD51), which is thought to be involved in the activation of TGF-β (fig. S6). Therefore, the source of TGF-β and its activation may be due to multiple cell types in vivo, and it is possible that the cells that produce TGF-β are different from those that activate it. In a previous study, α_vβ_8 integrins on T_regs were shown to be involved in the release of active TGF-β from latent TGF-β–glycoprotein A repetitions predominant (GARP) complexes on the surface of T_regs (23), suggesting that this may be a key mechanism by which they suppress. We found that pretreatment of sorted T_regs with anti–TGF-β antibodies to block TGF-β only on the surface of T_regs, before their addition to collagen-fibrin gel cultures containing either T_reg-depleted tumors or cultured B16-OVA cells, abolished their ability to suppress (Fig. 6, C and D). In both cases, the killing efficiency of OT-1 T cells remained similar to that of the OT-1 T cells in the T_reg-depleted control (Tables 1 and 2). Together, these data suggest that surface-bound TGF-β on T_regs is responsible for suppressing the OT-1 cell–mediated killing of B16-OVA tumors in collagen-fibrin gels.

The suppressive effects of T_regs are reflected not only by the increase in the number of viable tumor cells remaining in the collagen-fibrin gels after 72 hours but also in qualitative phenotypic changes observed in the OT-1 CD8$^+$ T cells. OT-1 cells recovered from the gels of T_reg-depleted or anti–TGF-β–treated tumors had increased amounts of the cytolytic effector molecule granzyme B and decreased cell surface expression of the T cell exhaustion marker and immune checkpoint receptor PD-1 compared to OT-1 T cells from control tumors (Fig. 6D). When T_regs were added back, the OT-1 T cells exhibited decreased amounts of granzyme B, whereas their cell surface expression of PD-1 remained unchanged (Fig. 6D). We found a similar but subtle change in the abundances of PD-1 and granzyme B in the endogenous tumor-infiltrating CD8$^+$ T cells in the tumor microenvironment after the depletion of T_regs in vivo with DT (fig. S7).

agreement with the former hypothesis, we found that the abundance of TGF-β on the surface of intratumor T_regs was greater than that on to intratumoral CD4$^+$ effector cells or CD8$^+$ T cells (Fig. 6A). To fully reconcile the mechanism by which T_regs modulated T cell cytolytic function and confirm that T_regs alone were sufficient for the suppression observed, we sorted T_regs by fluorescence-activated cell sorting (FACS) from nondepleted tumors and added them back to T_reg-depleted tumors or to cultured B16-OVA cells. In addition, to determine whether soluble or membrane-bound TGF-β was responsible for the suppression, we pretreated a portion of these T_regs with blocking antibodies against surface-bound TGF-β. Adding 20,000 sorted T_regs (corresponding to a 1:25 T_reg–to–effector cell ratio) to collagen-fibrin gel cultures partially restored the suppression in T_reg-depleted tumors (Fig. 6B). This was associated with an about two- to threefold increase in the number of viable tumor cells that remained in the gels after 72 hours and a 40 to 50% decrease in the killing rate (Table 1). Although these data suggest that T_regs are the primary cause of immune inhibition in the melanoma microenvironment, they do not rule out the possibility that T_regs cooperate with other cells in the tumor to suppress CD8$^+$ T cell cytotoxicity. However, solely adding T_regs to cultured B16-OVA cells in collagen-fibrin gels was sufficient to partially suppress killing by OT-1 cells to an extent that was within the range seen in nondepleted tumors (Fig. 6C).

Although we found that TGF-β was expressed on the surface of T_regs, but not effector T cells, there are other immune cells (including myeloid cells) in the tumor microenvironment and periphery that are capable of

DISCUSSION

Here, we showed that collagen-fibrin gel cultures recapitulated the suppressive conditions of the in vivo tumor microenvironment. Single-cell suspensions of B16 tumors were resistant to killing by OT-1 CD8$^+$ T cells when they were embedded together in 3D collagen-fibrin gels, but not when the cells were cocultured in a 2D tissue culture plate. This suppression was due to a decrease in the killing efficiency of OT-1 T cells, as measured by the killing constant k, as well as a functionally exhausted state of the OT-1 T cells, as shown by the decreased amount of intracellular granzyme B and increased cell surface abundance of PD-1. In vivo depletion of T_regs in Foxp3-DTR mice reversed the suppression and restored the OT-1 cell–mediated killing of B16 tumor cells. We sorted T_regs from Foxp3-GFP mice and showed that the readdition of T_regs to
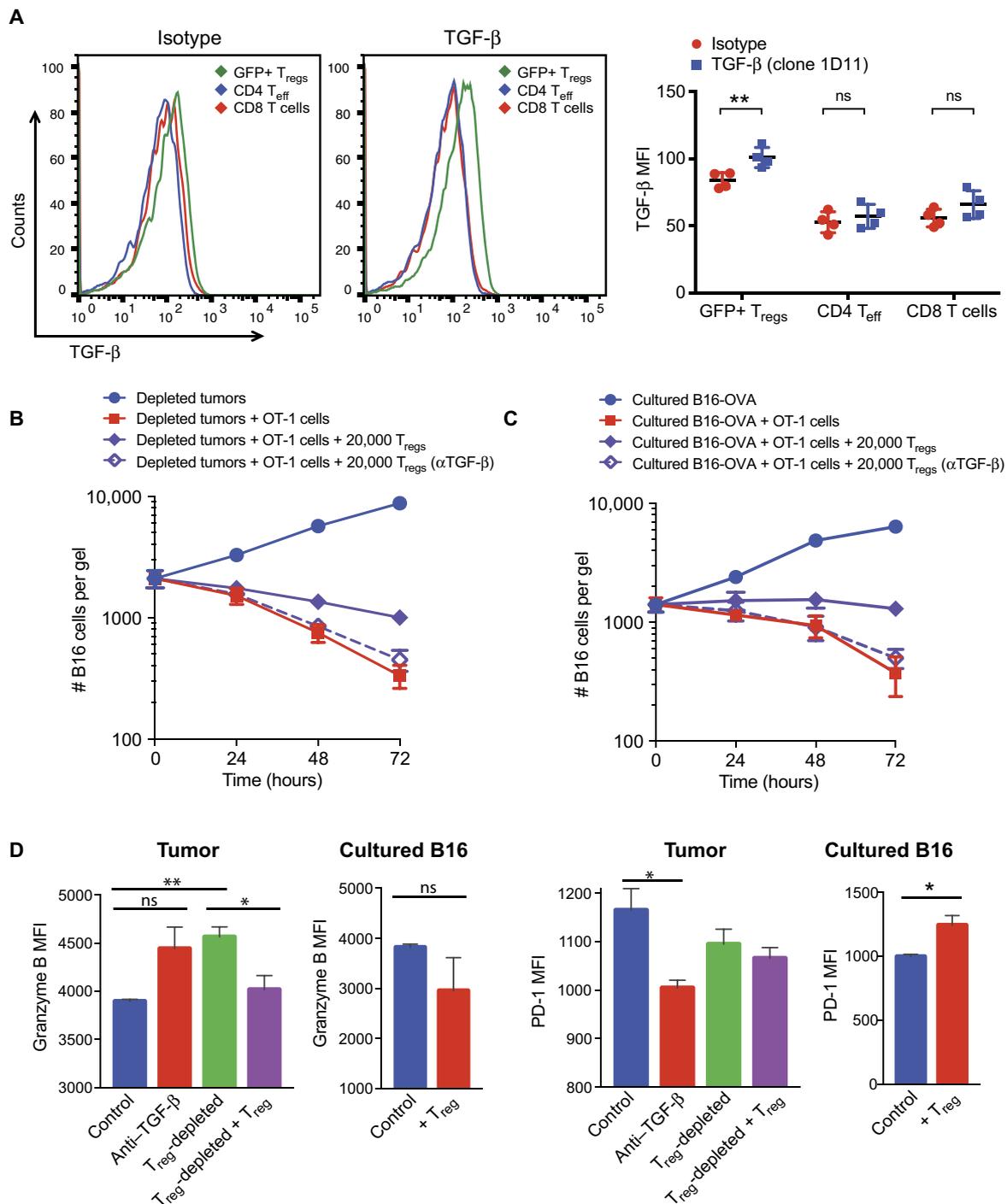
Fig. 6. Adding back T_regs to depleted tumors partially restored the suppression. (**A**) B16-OVA tumors from nondepleted mice were excised and dissociated as described in Materials and Methods. Left: The cell surface expression of TGF-β on CD4$^+$ effectors, CD8$^+$ T cells, and CD4$^+$Foxp3$^+$ (GFP$^+$) T_regs was assessed by flow cytometry. Representative histograms for the isotype control and anti–TGF-β antibody are shown. Right: Data represent the mean fluorescence intensity (MFI) ± SEM for TGF-β relative to that or an isotype control antibody for four mice per group. T_eff, effector T cell. (**B** and **C**) GFP$^+$ T_regs from tumors in Foxp3-GFP mice were sorted by FACS from nondepleted tumors and preincubated with blocking antibody against TGF-β. T_regs (2 × 10^4 cells) were then co-embedded with dissociated T_reg-depleted B16-OVA tumors (B) or cultured B16-OVA cells (C). At the indicated times, the gels were dissolved, and the numbers of the remaining B16 cells were measured using a clonogenic assay. Data are means ± SEM of the numbers of B16 cells from three experiments performed in duplicate. (**D**) OT-1 CD8$^+$ T cells were recovered from collagen-fibrin gels at 48 hours after culture under the indicated conditions and were analyzed by flow cytometry to determine the relative abundances of granzyme B (left) and PD-1 (right). Data are means ± SEM of the MFIs from triplicate analyses. *$P \leq 0.05$ and **$P \leq 0.01$.

T$_{reg}$-depleted tumors resulted in suppression of killing by CD8$^+$ T cells. Moreover, the addition of a blocking antibody to all three isoforms of TGF-β (clone 1D11) restored the CD8$^+$ T cell–mediated killing of B16 tumor cells. Intravital microscopy showed that adoptively transferred, antigen-specific CD8$^+$ T cells made direct contact with T$_{regs}$ in B16 tumors in vivo, suggesting that T$_{reg}$-mediated suppression of CD8$^+$ T cell function is contact- or proximity-dependent. Correspondingly, blocking TGF-β only on the surface of sorted T$_{regs}$ was sufficient to reverse their suppressive effect when they were added to T$_{reg}$-depleted tumors and cultured B16 cells. This finding suggests that surface-bound TGF-β on T$_{regs}$ is responsible for their suppressive effect. Together, these results suggest that T$_{regs}$ suppress killing by CD8$^+$ T cells in the tumor microenvironment in a contact- and TGF-β–dependent manner.

We did not observe suppression of CD8$^+$ T cell–mediated killing of dissociated tumors in assays performed in 2D 24-well plates (Fig. 2). This finding suggests that the presence of collagen and fibrin was necessary to confer T$_{reg}$-mediated suppression of CD8$^+$ T cell killing of dissociated tumors. It also highlights the importance of extracellular matrix proteins in sustaining the tumor microenvironment. Although collagen is the most abundant extracellular matrix protein found in most tissues, fibrin is a pathological matrix protein. Fibrin deposits have been described in several tumor types, including B16 melanomas (24, 25). This is presumably due to the leaky vessels found in tumors that enable blood components to enter the tumor bed. It is probable that the extracellular matrix components of the collagen-fibrin gels provide growth or beneficial signals (for example, through binding to cell surface integrins) to T$_{regs}$ and other immune cells that help to maintain their effector functions.

There have been several reports suggesting that T$_{regs}$ do not directly suppress effector T cell function in the tumor microenvironment in vivo but rather act through accessory cells such as APCs (8, 18, 26). In collagen-fibrin gel cocultures of dissociated B16 tumors, there are other immune cells present in addition to T$_{regs}$. Therefore, it is possible that other cells of the immune system aid T$_{regs}$ in their suppression. However, in a purified collagen-fibrin system containing only FACS-sorted T$_{regs}$ and cultured B16 melanoma cells, we found that T$_{regs}$ suppressed killing by OT-1 T cells (Fig. 6C); nonetheless, this suppressive effect was not as substantial as that observed in dissociated B16 tumors (Fig. 2B). This suggests that T$_{regs}$ alone are sufficient to confer the suppression; however, it does not rule out the possibility that T$_{regs}$ act in concert with other immune cells, such as APCs, to impart suppression of antitumor responses in vivo.

TGF-β has been widely demonstrated to play a fundamental role in immune tolerance. We found that blocking TGF-β with a monoclonal antibody was sufficient to reverse the suppression observed in collagen-fibrin cocultures (Fig. 4). The blocking antibody used, clone 1D11, blocks all three TGF-β (TGF-β1, TGF-β2, and TGF-β3) isoforms. We do not know which isoform(s) is responsible for immunosuppression, but TGF-β1 is the predominant isoform found in the immune system, and it has been implicated in antitumor immunity (23, 27, 28). Although most studies have focused on the secreted forms of TGF-β, several studies have demonstrated a role for surface-bound TGF-β on T$_{regs}$ in suppressing immune responses (19, 22). In agreement with these studies, we showed that blocking surface-bound TGF-β specifically on T$_{regs}$ reversed the suppressive ability of these T$_{regs}$ (Fig. 6, B and C). It is still unclear whether the surface-bound TGF-β is acting directly on T$_{regs}$ to maintain their suppressive activity or whether it suppresses CD8$^+$ T cells directly in a contact-dependent manner.

The synthesis, secretion, and processing of TGF-β are a complex, multistep process. Many cell types have the ability to produce and secrete the inactive form of TGF-β, which is then processed through several mecha-nisms involving extracellular matrix proteins, integrins, and proteases (29). Accordingly, it was suggested that the suppressive functions of TGF-β are mediated by modulating the extent of activation of TGF-β rather than its production (29). In our experiments, we found that many cells in the tumor microenvironment had the ability to produce TGF-β (fig. S6); however, it remains unclear which cell(s) in the tumor are the main source of the TGF-β. It was previously reported that effector T cell–derived TGF-β, but not T$_{reg}$-derived TGF-β, is responsible for the suppression of antitumor immunity (27). We propose that, regardless of the source of TGF-β, T$_{regs}$ are involved in processing and activating TGF-β and that this occurs through interactions between integrins and GARP on the surface of T$_{regs}$ (23).

There have been several clinical studies examining the effects of blocking TGF-β and its signaling pathways in cancer patients (30). Our data suggest that targeting T$_{regs}$ in vivo might provide clinical benefit. An attractive approach to this is using immunotherapies that specifically deplete T$_{regs}$ from the tumor microenvironment without affecting T$_{regs}$ systemically (3, 6, 31). We previously demonstrated that targeting the T cell costimulatory molecule GITR with the monoclonal agonist antibody DTA-1 selectively depletes T$_{regs}$ from the tumor microenvironment without affecting peripheral T$_{regs}$ (3, 13). This therapy works partially by depleting T$_{regs}$ through Fc-mediated processes (32). In addition, we showed that DTA-1 alters the lineage stability of the remaining intratumor T$_{regs}$ and induces an inflammatory effector T cell phenotype (13). In experiments with collagen-fibrin gel cocultures of dissociated tumors, we found that treatment with DTA-1 was sufficient to reverse the suppression of CD8$^+$ T cell–mediated killing similarly to depleting T$_{regs}$ from the tumors (13). In addition to targeting T$_{regs}$, GITR immunotherapy enhances CD8$^+$ T cell effector function. Thus, this therapy removes the suppression in the tumor microenvironment while concurrently enhancing T cell effector function. Currently, multiple monoclonal antibodies against GITR are being evaluated in phase 1 clinical trials for melanoma and other malignancies. In addition to antibodies against GITR, other immunotherapies, such as antibodies against CTLA-4 and OX40 [also known as tumor necrosis factor receptor superfamily member 4 (TNFRS4) and CD134] (6, 7, 33, 34), deplete T$_{regs}$ and enhance effector T cell function alone or in combination with other therapies, which makes this type of therapy an attractive approach to treating cancers. Together, our findings highlight the clinical potential of targeting T$_{regs}$ and TGF-β to restore effector T cell function within the tumor microenvironment.

MATERIALS AND METHODS
Mice
Mouse experiments were performed in accordance with institutional guidelines under a protocol approved by the Memorial Sloan Kettering Cancer Center (MSKCC) Institutional Animal Care and Use Committee. All mice were maintained in a pathogen-free facility according to the National Institutes of Health Animal Care guidelines. C57BL/6J mice (females, 6 to 10 weeks old) and OT-1 TCR transgenic mice (35) were purchased from The Jackson Laboratory. Pmel-1 TCR transgenic mice (36) were obtained from N. Restifo (National Institutes of Health). Foxp3-GFP knock-in mice were a gift from A. Rudensky (MSKCC). Foxp3-DTR (Foxp3-GDL) mice were a gift from G. Hämmerling [Deutsches Krebsforschungszentrum (DKFZ)]. CCR2-DTR mice were generated by T. Hohl (MSKCC).

Cell lines and tumor challenge
The B16-F10 mouse melanoma line was originally obtained from I. Fidler (MD Anderson Cancer Center, Houston, TX). These cells

Table 1. Calculation of k values for T_{reg}-depleted tumors. The value of k (min) for each condition was calculated from the equation $b_t = b_0 e^{-kpt+gt}$ and the values obtained in Fig. 6B. The percentage decreases compared to T_{reg}-depleted tumors at each time point are listed in parentheses.

Time (hours)	T_{reg}-depleted tumor	T_{reg}-depleted tumor + T_{regs}	T_{reg}-depleted tumor + T_{regs} + anti–TGF-β
24	0.77×10^{-9}	0.66×10^{-9}	0.66×10^{-9}
48	1.44×10^{-9}	0.84×10^{-9} (42%)	1.41×10^{-9} (2%)
72	1.79×10^{-9}	0.88×10^{-9} (51%)	1.40×10^{-9} (21%)

Table 2. Calculation of k values for cultured B16-OVA cells. The value of k (min) for each condition was calculated from the equation $b_t = b_0 e^{-kpt+gt}$ and the values obtained in Fig. 6C. The percentage changes compared to B16-OVA cells alone at each time point are listed in parentheses.

Time (hours)	B16-OVA cells	B16-OVA + T_{regs}	B16-OVA + T_{regs} + anti–TGF-β
24	0.69×10^{-9}	0.74×10^{-9}	1.07×10^{-9}
48	0.94×10^{-9}	0.19×10^{-9} (−80%)	0.74×10^{-9} (−21%)
72	1.60×10^{-9}	0.93×10^{-9} (−42%)	1.68×10^{-9} (+5%)

were maintained in RPMI 1640 containing 7.5% fetal bovine serum (FBS) and L-glutamine. B16-F10 cells were transfected with plasmid encoding full-length OVA protein to generate B16-OVA cells as previously described (37). YFP-B16 cells used for the imaging experiments were generated as previously described (10). Tumor cells were maintained in RPMI 1640 containing 7.5% FBS. For B16-OVA and YFP-B16 cells, the growth medium was supplemented with G418 (0.5 mg/ml). For tumor challenge experiments, 1×10^5 viable B16-OVA cells in 100 μl of phosphate-buffered saline (PBS) were injected intradermally into the right flank of C57BL/6 mice. For ex vivo analysis of immune infiltrates, mice were injected subcutaneously with the indicated numbers of tumor cells reconstituted in 150 μl of growth factor–reduced Matrigel (BD Biosciences).

In vitro activation of OT-1 and Pmel CD8⁺ T cells
OT-1 CD8⁺ T cells express a transgene encoding a TCR that specifically recognizes the OVA peptide (Ser-Ile-Ile-Asn-Phe-Glu-Lys-Leu) in the context of mouse MHC I H-2k^b (35). Pmel-1 CD8⁺ T cells express a transgene encoding a TCR that specifically recognizes the Pmel-1 (gp100) peptide (Glu-Gly-Ser-Arg-Asn-Gln-Asp-Trp-Leu) in the context of mouse MHC I H-2D^b (36). Activated OT-1 or Pmel-1 T cells were generated by incubation of peptide-pulsed mouse splenocytes (5×10^6 cells/ml) in vitro for 5 to 7 days in the presence of IL-2. Briefly, a mouse spleen was homogenized to generate a single-cell suspension, and the released cells were pelleted and resuspended in 3 ml of ACK lysis buffer (Lonza) for 1 min to lyse red blood cells. The splenocytes were washed, resuspended at 5×10^6 cells/ml in T cell growth medium [RPMI 1640, penicillin (100 U/ml), streptomycin (100 mg/ml), 10% FBS, 2 mM L-glutamine, 50 μM 2-mercaptoethanol, and 1 mM sodium pyruvate] containing OVA peptide or gp100 peptide (0.75 μg/ml), and incubated at 37°C in a 95% air and 5% CO_2 humidified atmosphere. On days 3 and 5, 25 ml of fresh T cell growth medium containing recombinant mouse IL-2 (20 U/ml; eBioscience) was added to the cultures. On day 7, viable cells were purified by centrifugation at 400g for 30 min at room temperature over a Histopaque gradient (density, 1.083; Sigma-Aldrich). This method yielded antigen-specific CD8⁺ T cells that were 90 to 95% tetramer⁺ for their respective peptides.

Collagen-fibrin gel killing assay
The collagen-fibrin gel-based killing assay has been previously described in depth (11). We adapted this assay to examine the killing of ex vivo B16 tumors. Briefly, C57BL/6 mice (6 to 8 weeks old) were tumor-challenged with 1×10^5 viable B16-OVA cells intradermally on the right flank. Tumors were excised on day 10 or 11 and

dissected into smaller pieces. The tumors were then incubated for 5 min with collagenase (250 μg/ml) in PBS containing Ca^{2+} and Mg^{2+} before being homogenized through 70-μm mesh cell strainers to generate single-cell suspensions. The number of viable tumor cells and immune infiltrates was assessed using a hemocytometer and trypan blue exclusion. The fraction of immune infiltrates within the dissociated tumors was confirmed by flow cytometry with an anti-CD45 antibody. Viable tumor cells (1×10^4; together with all infiltrating cells) were co-embedded with or without 5×10^5 in vitro–activated CD8⁺ T cells into collagen-fibrin gels (0.1-ml volume). As a control for each experiment, 1×10^4 viable B16-OVA cells cultured in vitro were also co-embedded with or without 5×10^5 in vitro–activated CD8⁺ T cells in collagen-fibrin gels. Duplicate gels were lysed daily with collagenase and trypsin for up to 3 days. The viable tumor cells from dissolved gels were diluted and plated in six-well plates for colony formation. Seven days later, plates were fixed with 3.7% formaldehyde and stained with 2% methylene blue. Colonies were manually counted to assess the number of cells. For experiments in which CD8⁺ T cells were analyzed by flow cytometry, collagen-fibrin gels were lysed with collagenase only, which was followed by mechanical pipetting to fully dissolve the gels and recover single-cell suspensions of T cells.

Depleting T_{regs} in vivo
In experiments in which DT was used to deplete immune cell subsets in vivo, Foxp3-DTR and CCR2-DTR mice were injected intraperitoneally with 45 ng of DT in 0.2 ml of PBS for the depletion of either Foxp3⁺ cells or CCR2⁺ cells, respectively. For all experiments, DT was administered on day 8 or 9 after tumor inoculation, and tumors were excised 48 hours later.

Calculating the value for k
k was calculated according to the following equation: $bt = b0\, e^{-kpt+gt}$ where bt is the concentration of B16 cells at time t, $b0$ is the concentration of B16 cells at time 0, k is the killing rate constant (or killing efficiency) for CD8⁺ T cells, p is the concentration of CD8⁺ T cells, and g is the growth rate constant for B16 cells (11). Experimentally determined values were used to calculate k.

Purification of T_{regs}
In some experiments, T_{regs} were purified with MACS beads. B16-OVA tumors were excised on day 10 or 11 after tumor challenge and were dissociated as described earlier. T_{regs} were purified from dissociated tumors in vitro by magnetic bead separation with the CD4⁺CD25⁺

Regulatory T Cell Isolation Kit (Miltenyi). The purity of these cells was confirmed by flow cytometric analysis with fluorophore-conjugated antibodies against CD4, CD25, and Foxp3. In other experiments, T_{regs} were purified by FACS. Foxp3-GFP mice were challenged with 1×10^5 B16-OVA tumor cells. On day 10 or 11, the B16-OVA tumors were excised and dissociated as described earlier. T_{regs} were sorted on the basis of viable CD4$^+$ GFP$^+$ cells on a Cytomation MoFlo or BD FACSAria cell sorter in the MSKCC Flow Cytometry Core Facility.

Flow cytometric analysis of cell surface antigens and intracellular proteins

Cell suspensions were incubated in Fc block (anti-CD16 and anti-CD32 antibodies; BD Biosciences) for 20 min on ice in FACS buffer (PBS containing 0.5% bovine serum albumin and 2 mM EDTA) before being stained for cell surface markers. Samples were incubated with fluorophore-conjugated antibodies against CD4, CD8, CD25, PD-1, and TGF-β (clone 1D11) for 20 to 30 min and then were washed three times with FACS buffer. The Foxp3 Staining Kit (eBioscience) was used for the intracellular staining of Foxp3 and granzyme B. Dead cells were excluded from the analysis with the Fixable Viability Dye eFluor 506 (eBioscience). Samples were acquired on a 12-color LSR II flow cytometer, and data were analyzed with FlowJo software (Tree Star).

Intravital imaging

YFP-B16 tumors were injected in the left flank of either WT or Foxp3-GFP mice upstream of the inguinal LN. The mice were imaged at multiple time points to find the time of maximal infiltration and compensate for variability associated with each set of tumor injections, priming response, and 3D tumor structures. Seven days after the transfer of fluorescently labeled CD8$^+$ T cells, the mice were anesthetized with 1.5% isoflurane given concurrently with O_2 (1 liter/min). Each mouse was then placed on a heated platform maintained at 37°C. Surgery was performed to open up a skin flap, extending from the forelimbs to the hindlimbs, up to the ventral midline, exposing the tumor and inguinal LN while maintaining vasculature integrity. The tumor and TDLN were then isolated under nylon washer–mounted coverslips with PBS and visualized with a heated (37°C) water dipping 40× objective lens (Nikon). The temperature of the isolated tissues was checked with a thermal probe to ensure that it was maintained at 37°C. Time-lapse images were acquired with a Z-depth on the average of 100 to 150 μm with 3 μm between steps, starting at ±10 μm from the top edge of the tumor cells. Mosaic images were taken with 50-μm overlaps between adjacent regions. The video capture rate of more than 20 fps enabled 6:1 frame averaging with a sample area that included up to nine adjacent 270-μm × 270-μm × 100-μm volumes to produce a mosaic image every 80 to 120 s. Time-lapse images varied in length from 60 to 240 min with mosaic images taken for as long as possible.

Image analysis

Images were analyzed with Volocity 4.0.2 software (Improvision) and custom-developed MATLAB code. Mosaic images were compiled together with MATLAB before being imported into Volocity. T cell tracking was performed on individual quadrants in Volocity. Images were corrected for contrast with $3 \times 3 \times 3$–pixel noise filtering to remove background signal where necessary. Tracks were calculated with Volocity automatic object acquisition and tracking modules and were verified for algorithmic errors. Image drift was removed from the calculated trajectory and velocity measurements by calculating the average movement for three tumor landmarks per image during the time lapse and adjusting the cell tracking measurement accordingly. Intratumor T cell positions were calculated by producing a high digital threshold map of the tumor images and then comparing Volocity-calculated cell centroid positions with the tumor map to determine cell location with respect to tumor or "not tumor" using MATLAB. Statistical comparisons of Pmel-1 versus OT-1 were performed with GraphPad Prism 5 software with a Student's t test.

T_{reg} cell proximity and contact score generation

During the verification of trajectory measurements for Pmel-1 T cells in Foxp3-GFP mice, each cell was manually assessed in XY and Z for interactions with T_{regs}. Cells received a score of 1 for each contact with or proximity to (within 10 μm) each T_{reg}, with additional interactions per time point being additive. Scores were normalized by dividing the sum of the interactions by the number of time points for which an individual cell was tracked. Scores produced were weighted time average.

Statistical analysis

Unless otherwise indicated, all experiments were performed at least three times with duplicate samples. Data were reported as means ± SEM for the number of experiments indicated. For statistical analyses, a Kruskal-Wallis test (nonparametric equivalent of analysis of variance) was applied when there were more than two groups. If statistically significant, pairwise comparisons with Wilcoxon test and Bonferroni correction for multiple comparisons were applied.

SUPPLEMENTARY MATERIALS

www.sciencesignaling.org/cgi/content/full/10/494/eaak9702/DC1

Summary of statistical analyses

Fig. S1. Analysis of immune cell infiltrates in tumors from DT-treated Foxp3-DTR mice.

Fig. S2. In vivo depletion of CCR2$^+$ cells in CCR2-DTR mice has no effect on the suppression of CD8$^+$ T cell–mediated killing by the tumor microenvironment.

Fig. S3. Depleting T_{regs} ex vivo with anti-CD25 MicroBeads has no effect on the immunosuppression of CD8$^+$ T cells.

Fig. S4. T_{regs} cause minor alterations to the mobility of CD8$^+$ T cells in the tumor.

Fig. S5. Suppression of CD8$^+$ T cells by T_{regs} is contact- or proximity-dependent.

Fig. S6. Expression of TGF-β and CD51 ($α_V$ integrin) in immune cell subsets from the tumors and spleens of B16 tumor–bearing mice.

Fig. S7. Effect of DT on the expression of PD-1 and granzyme B on the surface of endogenous CD8$^+$ T cells.

Movie S1. CFP-Pmel T cells are found in regions highly infiltrated by T_{regs}.

Movie S2. CFP-Pmel T cells are found within proximity to or make contact with T_{regs}.

REFERENCES AND NOTES

1. D. Mittal, M. M. Gubin, R. D. Schreiber, M. J. Smyth, New insights into cancer immunoediting and its three component phases—Elimination, equilibrium and escape. *Curr. Opin. Immunol.* **27**, 16–25 (2014).

2. R. D. Schreiber, L. J. Old, M. J. Smyth, Cancer immunoediting: Integrating immunity's roles in cancer suppression and promotion. *Science* **331**, 1565–1570 (2011).

3. A. D. Cohen, D. A. Schaer, C. Liu, Y. Li, D. Hirschhorn-Cymmerman, S. C. Kim, A. Diab, G. Rizzuto, F. Duan, M. A. Perales, T. Merghoub, A. N. Houghton, J. D. Wolchok, Agonist anti-GITR monoclonal antibody induces melanoma tumor immunity in mice by altering regulatory T cell stability and intra-tumor accumulation. *PLOS ONE* **5**, e10436 (2010).

4. K. Klages, C. T. Mayer, K. Lahl, C. Loddenkemper, M. W. L. Teng, S. F. Ngiow, M. J. Smyth, A. Hamann, J. Huehn, T. Sparwasser, Selective depletion of Foxp3$^+$ regulatory T cells improves effective therapeutic vaccination against established melanoma. *Cancer Res.* **70**, 7788–7799 (2010).

5. X. Li, E. Kostareli, J. Suffner, N. Garbi, G. J. Hämmerling, Efficient Treg depletion induces T-cell infiltration and rejection of large tumors. *Eur. J. Immunol.* **40**, 3325–3335 (2010).

6. D. Hirschhorn-Cymerman, G. A. Rizzuto, T. Merghoub, A. D. Cohen, F. Avogadri, A. M. Lesokhin, A. D. Weinberg, J. D. Wolchok, A. N. Houghton, OX40 engagement and

chemotherapy combination provides potent antitumor immunity with concomitant regulatory T cell apoptosis. *J. Exp. Med.* **206**, 1103–1116 (2009).

7. S. A. Quezada, K. S. Peggs, M. A. Curran, J. P. Allison, CTLA4 blockade and GM-CSF combination immunotherapy alters the intratumor balance of effector and regulatory T cells. *J. Clin. Invest.* **116**, 1935–1945 (2006).

8. A. Schmidt, N. Oberle, P. H. Krammer, Molecular mechanisms of Treg-mediated T cell suppression. *Front. Immunol.* **3**, 51 (2012).

9. A. Schmidt, N. Oberle, E.-M. Weiß, D. Vobis, S. Frischbutter, R. Baumgrass, C. S. Falk, M. Haag, B. Brügger, H. Lin, G. W. Mayr, P. Reichardt, M. Gunzer, E. Suri-Payer, P. H. Krammer, Human regulatory T cells rapidly suppress T cell receptor–induced Ca^{2+}, NF-κB, and NFAT signaling in conventional T cells. *Sci. Signal.* **4**, ra90 (2011).

10. D. A. Schaer, Y. Li, T. Merghoub, G. A. Rizzuto, A. Shemesh, A. D. Cohen, Y. Li, F. Avogadri, R. Toledo-Crow, A. N. Houghton, J. D. Wolchok, Detection of intra-tumor self antigen recognition during melanoma tumor progression in mice using advanced multimode confocal/two photon microscope. *PLOS ONE* **6**, e21214 (2011).

11. S. Budhu, J. D. Loike, A. Pandolfi, S. Han, G. Catalano, A. Constantinescu, R. Clynes, S. C. Silverstein, CD8$^+$ T cell concentration determines their efficiency in killing cognate antigen–expressing syngeneic mammalian cells in vitro and in mouse tissues. *J. Exp. Med.* **207**, 223–235 (2010).

12. A. M. Lesokhin, T. M. Hohl, S. Kitano, C. Cortez, D. Hirschhorn-Cymerman, F. Avogadri, G. A. Rizzuto, J. J. Lazarus, E. G. Pamer, A. N. Houghton, T. Merghoub, J. D. Wolchok, Monocytic CCR2$^+$ myeloid-derived suppressor cells promote immune escape by limiting activated CD8 T-cell infiltration into the tumor microenvironment. *Cancer Res.* **72**, 876–886 (2012).

13. D. A. Schaer, S. Budhu, C. Liu, C. Bryson, N. Malandro, A. Cohen, H. Zhong, X. Yang, A. N. Houghton, T. Merghoub, J. D. Wolchok, GITR pathway activation abrogates tumor immune suppression through loss of regulatory T-cell lineage stability. *Cancer Immunol. Res.* **1**, 320–331 (2013).

14. M.-L. Chen, M. J. Pittet, L. Gorelik, R. A. Flavell, R. Weissleder, H. von Boehmer, K. Khazaie, Regulatory T cells suppress tumor-specific CD8 T cell cytotoxicity through TGF-β signals in vivo. *Proc. Natl. Acad. Sci. U.S.A.* **102**, 419–424 (2005).

15. L. W. Collison, V. Chaturvedi, A. L. Henderson, P. R. Giacomin, C. Guy, J. Bankoti, D. Finkelstein, K. Forbes, C. J. Workman, S. A. Brown, J. E. Rehg, M. L. Jones, H.-T. Ni, D. Artis, M. J. Turk, D. A. A. Vignali, IL-35-mediated induction of a potent regulatory T cell population. *Nat. Immunol.* **11**, 1093–1101 (2010).

16. X. Cao, S. F. Cai, T. A. Fehniger, J. Song, L. I. Collins, D. R. Piwnica-Worms, T. J. Ley, Granzyme B and perforin are important for regulatory T cell-mediated suppression of tumor clearance. *Immunity* **27**, 635–646 (2007).

17. L. Gorelik, R. A. Flavell, Immune-mediated eradication of tumors through the blockade of transforming growth factor-β signaling in T cells. *Nat. Med.* **7**, 1118–1122 (2001).

18. T. R. Mempel, M. J. Pittet, K. Khazaie, W. Weninger, R. Weissleder, H. von Boehmer, U. H. von Andrian, Regulatory T cells reversibly suppress cytotoxic T cell function independent of effector differentiation. *Immunity* **25**, 129–141 (2006).

19. K. Nakamura, A. Kitani, W. Strober, Cell contact–dependent immunosuppression by CD4$^+$CD25$^+$ regulatory T cells is mediated by cell surface–bound transforming growth factor β. *J. Exp. Med.* **194**, 629–644 (2001).

20. J. D. Fontenot, J. P. Rasmussen, M. A. Gavin, A. Y. Rudensky, A function for interleukin 2 in Foxp3-expressing regulatory T cells. *Nat. Immunol.* **6**, 1142–1151 (2005).

21. A. L. Smith, T. P. Robin, H. L. Ford, Molecular pathways: Targeting the TGF-β pathway for cancer therapy. *Clin. Cancer Res.* **18**, 4514–4521 (2012).

22. M. Smith, C. Seguin-Devaux, T. B. Oriss, B. Dixon-McCarthy, L. Yang, B. T. Ameredes, T. E. Corcoran, A. Ray, Tolerance induced by inhaled antigen involves CD4$^+$ T cells expressing membrane-bound TGF-β and FOXP3. *J. Clin. Invest.* **114**, 28–38 (2004).

23. J. P. Edwards, A. M. Thornton, E. M. Shevach, Release of active TGF-β1 from the latent TGF-β1/GARP complex on T regulatory cells is mediated by integrin β$_8$. *J. Immunol.* **193**, 2843–2849 (2014).

24. J. Dewever, F. Frerart, C. Bouzin, C. Baudelet, R. Ansiaux, P. Sonveaux, B. Gallez, C. Dessy, O. Feron, Caveolin-1 is critical for the maturation of tumor blood vessels through the regulation of both endothelial tube formation and mural cell recruitment. *Am. J. Pathol.* **171**, 1619–1628 (2007).

25. H. F. Dvorak, J. A. Nagy, J. B. Berse, L. F. Brown, K.-T. Yeo, T.-K. Yeo, A. M. Dvorak, L. van de Water, T. M. Sioussat, D. R. Senger, Vascular permeability factor, fibrin, and the pathogenesis of tumor stroma formation. *Ann. N. Y. Acad. Sci.* **667**, 101–111 (1992).

26. C. A. Bauer, E. Y. Kim, F. Marangoni, E. Carrizosa, N. M. Claudio, T. R. Mempel, Dynamic Treg interactions with intratumoral APCs promote local CTL dysfunction. *J. Clin. Invest.* **124**, 2425–2440 (2014).

27. M. K. Donkor, A. Sarkar, P. A. Savage, R. A. Franklin, L. K. Johnson, A. A. Jungbluth, J. P. Allison, M. O. Li, T cell surveillance of oncogene-induced prostate cancer is impeded by T cell-derived TGF-β1 cytokine. *Immunity* **35**, 123–134 (2011).

28. D. Q. Tran, J. Andersson, R. Wang, H. Ramsey, D. Unutmaz, E. M. Shevach, GARP (LRRC32) is essential for the surface expression of latent TGF-β on platelets and activated FOXP3$^+$ regulatory T cells. *Proc. Natl. Acad. Sci. U.S.A.* **106**, 13445–13450 (2009).

29. M. A. Travis, D. Sheppard, TGF-β activation and function in immunity. *Annu. Rev. Immunol.* **32**, 51–82 (2014).

30. C. Neuzillet, A. Tijeras-Raballand, R. Cohen, J. Cros, S. Faivre, E. Raymond, A. de Gramont, Targeting the TGFβ pathway for cancer therapy. *Pharmacol. Ther.* **147**, 22–31 (2015).

31. T. R. Simpson, F. Li, W. Montalvo-Ortiz, M. A. Sepulveda, K. Bergerhoff, F. Arce, C. Roddie, J. Y. Henry, H. Yagita, J. D. Wolchok, K. S. Peggs, J. V. Ravetch, J. P. Allison, S. A. Quezada, Fc-dependent depletion of tumor-infiltrating regulatory T cells co-defines the efficacy of anti–CTLA-4 therapy against melanoma. *J. Exp. Med.* **210**, 1695–1710 (2013).

32. Y. Bulliard, R. Jolicoeur, M. Windman, S. M. Rue, S. Ettenberg, D. A. Knee, N. S. Wilson, G. Dranoff, J. L. Brogdon, Activating Fc γ receptors contribute to the antitumor activities of immunoregulatory receptor-targeting antibodies. *J. Exp. Med.* **210**, 1685–1693 (2013).

33. F. Avogadri, R. Zappasodi, A. Yang, S. Budhu, N. Malandro, D. Hirschhorn-Cymerman, S. Tiwari, M. F. Maughan, R. Olmsted, J. D. Wolchok, T. Merghoub, Combination of alphavirus replicon particle–based vaccination with immunomodulatory antibodies: Therapeutic activity in the B16 melanoma mouse model and immune correlates. *Cancer Immunol. Res.* **2**, 448–458 (2014).

34. D. Hirschhorn-Cymerman, S. Budhu, S. Kitano, C. Liu, F. Zhao, H. Zhong, A. M. Lesokhin, F. Avogadri-Connors, J. Yuan, Y. Li, A. N. Houghton, T. Merghoub, J. D. Wolchok, Induction of tumoricidal function in CD4$^+$ T cells is associated with concomitant memory and terminally differentiated phenotype. *J. Exp. Med.* **209**, 2113–2126 (2012).

35. K. A. Hogquist, S. C. Jameson, W. R. Heath, J. L. Howard, M. J. Bevan, F. R. Carbone, T cell receptor antagonist peptides induce positive selection. *Cell* **76**, 17–27 (1994).

36. W. W. Overwijk, M. R. Theoret, S. E. Finkelstein, D. R. Surman, L. A. de Jong, F. A. Vyth-Dreese, T. A. Dellemijn, P. A. Antony, P. J. Spiess, D. C. Palmer, D. M. Heimann, C. A. Klebanoff, Z. Yu, L. N. Hwang, L. Feigenbaum, A. M. Kruisbeek, S. A. Rosenberg, N. P. Restifo, Tumor regression and autoimmunity after reversal of a functionally tolerant state of self-reactive CD8$^+$ T cells. *J. Exp. Med.* **198**, 569–580 (2003).

37. L. D. Falo Jr., M. Kovacsovics-Bankowski, K. Thompson, K. L. Rock, Targeting antigen into the phagocytic pathway in vivo induces protective tumour immunity. *Nat. Med.* **1**, 649–653 (1995).

Science Signaling

Blockade of surface-bound TGF-β on regulatory T cells abrogates suppression of effector T cell function in the tumor microenvironment

Sadna Budhu, David A. Schaer, Yongbiao Li, Ricardo Toledo-Crow, Katherine Panageas, Xia Yang, Hong Zhong, Alan N. Houghton, Samuel C. Silverstein, Taha Merghoub and Jedd D. Wolchok

Blocking immunosuppression

The antitumor effects of CD8$^+$ T cells can be blocked in the tumor microenvironment, including through the suppressive function of regulatory T cells (T$_{regs}$). Standard in vitro systems fail to recapitulate the conditions that immune cells are exposed to in vivo. Budhu *et al.* used a three-dimensional, collagen-fibrin gel system to investigate the effects of CD8$^+$ T cells on cocultured melanoma cells excised from mouse tumors. The antitumor activity of the CD8$^+$ T cells was inhibited by the presence of tumor-derived T$_{regs}$, which depended on cell-cell contact or close proximity, required the cytokine TGF-β on the T$_{reg}$ cell surface, and resulted in the increased cell surface expression of the immune checkpoint receptor PD-1 on the CD8$^+$ T cells. A blocking antibody against TGF-β prevented immunosuppression, suggesting a therapeutic strategy to inhibit T$_{reg}$ activity in tumors.

ARTICLE TOOLS	http://stke.sciencemag.org/content/10/494/eaak9702
SUPPLEMENTARY MATERIALS	http://stke.sciencemag.org/content/suppl/2017/08/25/10.494.eaak9702.DC1
RELATED CONTENT	http://stke.sciencemag.org/content/sigtrans/10/491/eaao5803.full http://stke.sciencemag.org/content/sigtrans/8/407/ec370.abstract http://stke.sciencemag.org/content/sigtrans/8/396/ra97.full http://science.sciencemag.org/content/sci/348/6236/803.full http://stm.sciencemag.org/content/scitransmed/9/393/eaal4922.full http://stm.sciencemag.org/content/scitransmed/8/328/328rv4.full http://stke.sciencemag.org/content/sigtrans/10/495/eaap8364.full http://stke.sciencemag.org/content/sigtrans/10/500/eaam5353.full http://stke.sciencemag.org/content/sigtrans/10/506/eaar5179.full http://stke.sciencemag.org/content/sigtrans/10/509/eaar6885.full http://stke.sciencemag.org/content/sigtrans/11/511/eaan0790.full http://stke.sciencemag.org/content/sigtrans/11/511/eaar8122.full http://stke.sciencemag.org/content/sigtrans/11/531/eaau2250.full http://stke.sciencemag.org/content/sigtrans/11/546/eaar8371.full http://immunology.sciencemag.org/content/immunology/2/11/eaaj1738.full http://immunology.sciencemag.org/content/immunology/2/11/eaai7911.full http://stke.sciencemag.org/content/sigtrans/12/601/eaaz4717.full
REFERENCES	This article cites 37 articles, 17 of which you can access for free http://stke.sciencemag.org/content/10/494/eaak9702#BIBL